IEEE Access
Multidisciplinary | Rapid Review | Open Access Journal

Received 14 August 2023, accepted 3 September 2023, date of publication 7 September 2023,
date of current version 14 September 2023.

Digital Object Identifier 10.1109/ACCESS.2023.3312722

RESEARCH ARTICLE

Impact of Geomagnetically Induced Current on Power Grid Resiliency Under Extreme Geomagnetic Disturbance

ZMNAKO MOHAMMED KHURSHID[1,2], NUR FADILAH AB AZIZ[1], (Member, IEEE), ZETI AKMA RHAZALI[1], AND MOHD ZAINAL ABIDIN AB KADIR[2], (Senior Member, IEEE)

[1]Institute of Power Engineering (IPE), Universiti Tenaga Nasional, Jalan IKRAM-UNITEN, Kajang, Selangor 43000, Malaysia
[2]Advanced Lightning, Power and Energy Research Centre (ALPER), Faculty of Engineering, Universiti Putra Malaysia, Serdang, Selangor 43400, Malaysia

Corresponding author: Nur Fadilah Ab Aziz (nfadilah@uniten.edu.my)

This work was supported in part by the Ministry of Higher Education (MOHE) of Malaysia under Grant FRGS/1/2018/TK04/UNITEN/02/6; in part by Tenaga Nasional Berhad (TNB) and University Tenaga Nasional (UNITEN), through the BOLD Refresh Publication Fund under Project J510050002-IC-6 and Project BOLDREFRESH2025-Centre of Excellence; and in part by Universiti Putra Malaysia (UPM).

ABSTRACT With the global commitment to achieving net zero carbon emissions by 2050, the importance of transitioning to clean and efficient energy sources has become increasingly crucial. On this note, grid resiliency is crucial for sustainable energy supply because it ensures a reliable and uninterrupted flow of electricity from renewable sources to consumers. By withstanding and recovering quickly from disruptions, the grid can maintain a stable energy supply, support the integration of intermittent renewable sources, and meet the increasing demand for clean energy. This study presents a detailed case study of the extreme geomagnetic disturbance (GMD) impacts on high voltage (HV) power networks in Peninsular Malaysia. The GMD events arise from extreme conditions on the Sun due to solar activity and drive geomagnetically induced current (GIC) in power transmission lines and other technological conductor networks, causing half-cycle saturation of earthed transformers and leading to voltage-control problems or transformer failure. The power system model comprises 54 substations interconnected with 500 kV, 275 kV, and 132 kV transmission lines. The GIC was calculated through the system with respect to different extreme geoelectric field strengths and substation grounding resistance (GR) values using the nodal admittance matrix (NAM) method. The results showed that extreme GMD events can produce intense GIC values across the system, especially at substations located at the edge and middle of the power network, meaning that the Malaysian power grid is not immune to such events. The maximum GIC was obtained at substation 22 with a value of 896 A at field orientation 140°. Also, the results showed that when the GRs of the substations were decreased, the calculated GICs across the system increased.

INDEX TERMS Energy, extreme space weather, geomagnetic disturbances, geomagnetically induced current, high voltage transformers.

I. INTRODUCTION

Geomagnetic disturbances (GMD) events occur due to the interaction of charged material ejected from the Sun during solar activity and interact with Earth's magnetosphere. This interaction causes enhancement of the existing electric currents in the ionosphere and results in rapid time geomagnetic field variations [1], [2]. There are a few types of disturbances that drive geomagnetic storms, such as coronal mass ejection (CME), corotating interaction regions (CIRs), and interplanetary shocks [3], [4]. The geomagnetic field variations create surface geoelectric electric fields and cause low frequency (0.001–1 Hz) geomagnetically induced currents (GICs) flow into grounded technological

The associate editor coordinating the review of this manuscript and approving it for publication was Mehmet Alper Uslu.

conductors [5], [6] such as oil and gas pipelines, power networks, and railway [7], as illustrated in Fig. 1.

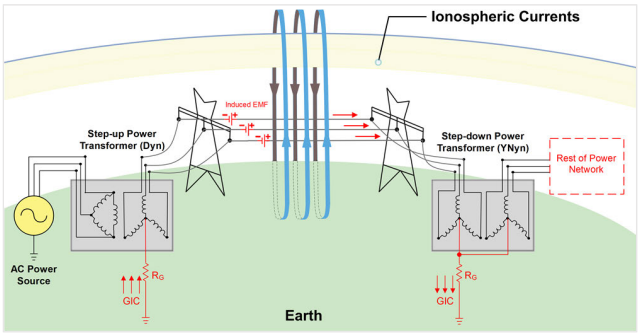

FIGURE 1. GIC event description in a power grid.

A neutral-grounded power transformer is most affected by GIC since it is built to work with alternating current (AC). The GIC flow through the windings of the transformer creates DC magnetic flux in the transformer's cores. The DC flux adds to the AC flux in a half cycle and subtracts in another, causing a half-cycle saturation due to the nonlinear response of the core material, as shown in Fig. 2.

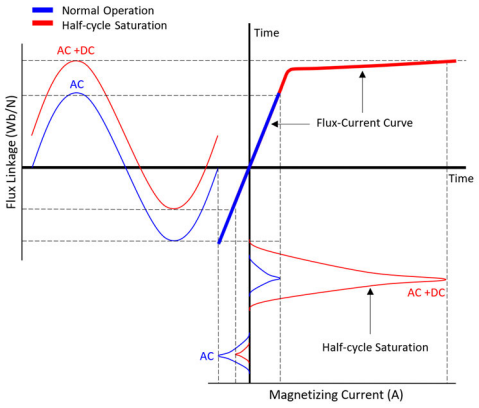

FIGURE 2. Magnetizing current of power transformer under normal operating condition and during half-cycle saturation.

When the transformer is operated during half-cycle saturation, it draws a large asymmetrical exciting current which is rich in even and odd harmonics and increases the reactive power losses of a transformer [8], [9], [10]. This asymmetrical current and the reactive power losses may result in hotspots in the transformer, relay misoperation, and tripping static var compensator (SVC), turning to permanent transformer damage or system blackout. The review of previous studies has shown that GMD effects can extend to power grids located in low latitudes as well and are not limited to high and mid-latitudes [7]. Therefore, we have made a few GIC analyses on the power network in Malaysia since it is located close to the equatorial electrojet (EEJ) [10], [11], [12]. In [10], we have analysed the GIC impacts on saturation of four high voltage (HV) transformers types available in the Malaysian power grid using AC analysis and proposed proper GIC blocking devices to mitigate the related impacts. In [11], we have analysed the effects of these devices on the potential power network ferroresonance. In [12], we have performed GIC analysis on the network with respect to benchmark geo-electric fields and the effects of lower voltage systems on the calculated GIC. This work shows the behaviour of the HV Malaysian power network under extreme GMD events. Even though the occurrence of extreme GMD events is rare, it can result in large GICs in the electric power grid that could affect system voltages, power transformer and system protection performance [13]. The analysis considered different parameters and scenarios, such as the effective GIC of transformers, substation isolation and grounding resistance (GR) on the calculated GIC. These parameters and characterization of such events are fundamental and vital to be carried out as the first time performed on the system to avoid the severe social and economic consequences and can present a clear view to power utility in case of any future space weather event. The rest of this paper is organized as follows. The Malaysian power network and related transformer data are introduced in the second section. The third section presents the method used to calculate GIC in the power grid. The fourth section includes the results and discussion of the simulation cases, and the fifth section is the conclusion.

II. POWER NETWORK MODEL

This work investigated the HV transmission network in Peninsular Malaysia under extreme GMD events, considering different scenarios. The system includes 117 HV transformers located in 54 substations. The stations are interconnected through 500 kV, 275 kV, and 132 kV transmission lines, as illustrated in Fig. 3. The transformer data is presented in Fig. 4. The k factor values in the figure were selected based on the recommendation of the North American Electric Reliability Corporation (NERC) standard since the actual value is unavailable and the system includes a large number of transformers [14].

III. GIC CALCULATION

The GIC is calculated across the system using the nodal admittance matrix (NAM) method, considering the DC equivalent model of the power network components since GIC is a quasi-dc current. For GIC calculations, any ungrounded transformer windings are excluded from the model since they do not have a path for GIC flow. The NAM method is widely used since it is relatively simple, straightforward, and requires a smaller number of equations to solve the circuit. To simplify a power network, a three-bus system example with a single-line diagram of the DC equivalent circuit of all components is used in Fig. 5, assuming that the resistance in each phase of each component in the circuit is equal.

where R_{T1} and R_{T2} are per-phase winding resistances of the transformers in nodes 1 and 2, respectively. R_s and R_c are per-phase series and common winding resistances of the autotransformer in node 3, respectively. R_{G1}, R_{G2}, and R_{G3} are GRs of the nodes 1, 2, and 3, respectively. R_{12} and R_{23}

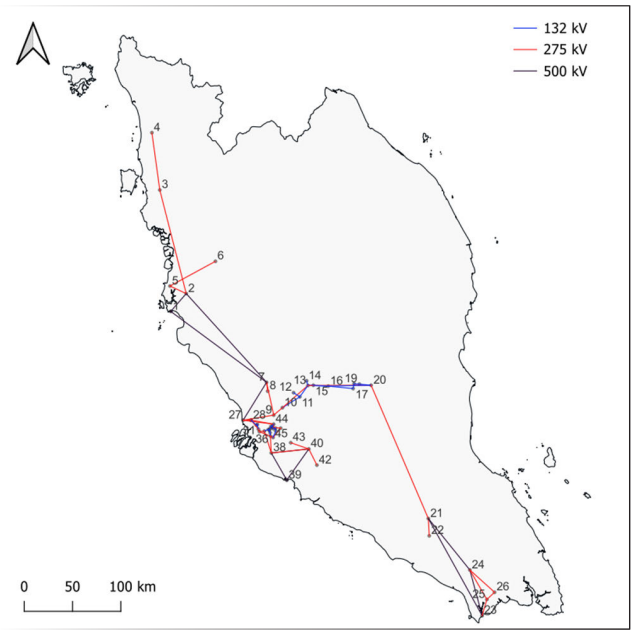

FIGURE 3. Description of the power network in Peninsular Malaysia.

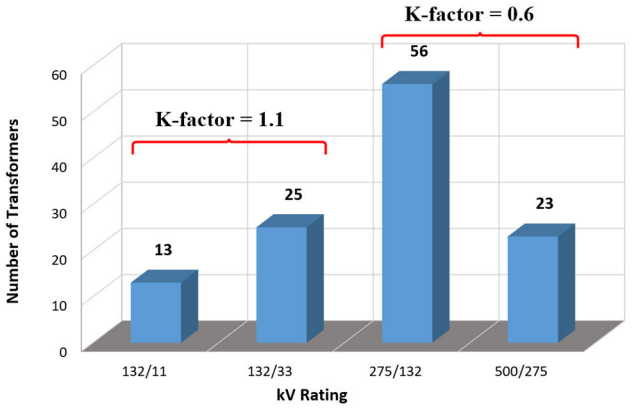

FIGURE 4. Transformer specification used in the power grid model.

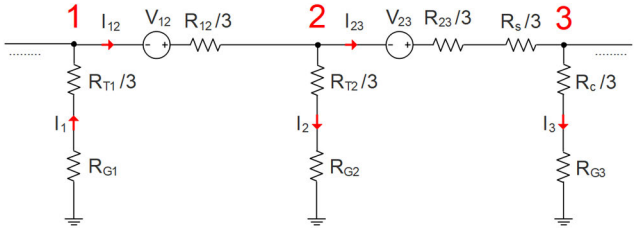

FIGURE 5. DC equivalent circuit of a three-bus network.

are per-phase line resistances between the nodes. I_{12} and I_{23} are current flow through the lines and I_1, I_2, and I_3 are current flow through the grounds of the nodes. V_{12} and V_{23} are the induced voltages along the lines, as presented in Equation (1).

$$V_{12} = E_x L_x + E_y L_y \tag{1}$$

where E_x and E_y are (V/km) uniform electric fields in the northward and eastward orientations, respectively and L_x and L_y are the corresponding northward and eastward line distances (km), respectively. In the NAM method, all voltage sources are transformed to current sources and all impedance elements are transformed to their equivalent admittances using Norton's theorem, as shown in Fig. 6.

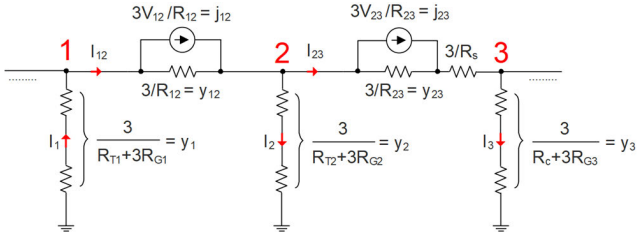

FIGURE 6. DC equivalent circuit of a three-bus network in nodal form.

where y_1, y_2 and y_3 are the node admittances, y_{12} and y_{23} are the transmission line admittances, and j_{12} and j_{23} are the equivalent current sources along the lines. The matrix of current sources is equal to

$$[Y][V] = [J] \tag{2}$$

where $[Y]$ is the network admittance matrix, $[V]$ is a $N \times 1$ vector of the nodal voltages, and $[J]$ is a $N \times 1$ vector of the current sources, as illustrated in matrix form in Equation (3).

$$\begin{pmatrix} Y_{11} & Y_{12} & \dots & Y_{1N} \\ Y_{21} & Y_{22} & \dots & Y_{2N} \\ \vdots & \ddots & \dots & \vdots \\ Y_{NN} & Y_{N2} & \dots & Y_{NN} \end{pmatrix} \begin{pmatrix} V_1 \\ V_2 \\ \vdots \\ V_N \end{pmatrix} = \begin{pmatrix} J_1 \\ J_2 \\ \vdots \\ J_N \end{pmatrix} \tag{3}$$

The nodal voltage is defined as:

$$[V] = [Y]^{-1}[J] \tag{4}$$

The GIC flow through the ground of the nodes in the power network is calculated as follows [15]:

$$[I_{GIC}] = ([1] + [Y][Z])^{-1}[J] \tag{5}$$

where [1] is a unit matrix and $[Z]$ is the earthing impedance matrix. The reactive power losses of the transformers under the GIC condition (Q_{GIC}) is calculated based on Equation (6).

$$Q_{GIC} = k \cdot I_{eff} + Q \tag{6}$$

where k is the reactive power/ampere scaling factor, which is dependent on the core type of transformer [16], [17] and I_{eff} is the effective value of the GIC flowing in the transformer windings and Q is reactive power losses of transformers at the normal operating condition without GIC. A detailed derivation of GIC calculation based on DC analysis was presented in [7].

IV. RESULTS AND DISCUSSION

The GIC analysis results were obtained from two main simulation cases considering different factors. The details of these cases are discussed in the following subsections.

A. FIRST SIMULATION CASE

In this simulation case, the power network vulnerability to GICs was performed taking into account the worst-case geomagnetic storm scenarios. The Malaysian power network model was subjected to extreme geoelectric fields with values of 5 V/km, 10 V/km, and 20 V/km in various angles of 0–180° clockwise directions starting from the North with an interval of 20° to investigate the effects of these field values on the system operation and reactive power losses. These selected geoelectric fields represent a 100-year storm scenario with different severity [18]. Approximately 5 V/km could occur during a severe GMD in certain regions where the earth's conductivity is high, whereas 10 V/km and 20 V/km could occur in regions with low earth conductivity [19]. In this case, the GR of the substations was fixed at 0.8 Ω as it is common to have substation GR less than 1 ohm in Malaysia due to its comprehensive/mesh earthing arrangement. This analysis would assist in estimating the power grid response under such extreme geoelectric fields and identify the most critical locations that may collapse due to such field strengths.

Firstly, we estimated the sum of effective GICs and corresponding reactive power losses of all transformers in the system with respect to applied field values. In Fig. 7, it can be seen that the highest sum of effective GICs for all transformers occurred at a 100° angle with the value of 601.12 A due to the 5 V/km geoelectric field which means a worse field angle with respect to the entire system as produces the highest GIC compared to other angles. Note that the effective GIC is the GIC that flows in the transformer windings. The corresponding reactive power loss for the same field value is 524.34 Mvar. When the applied geoelectric field was increased to 10 V/km, the results of effective GICs and reactive power were doubled to 1202.23 A and 1048.67 Mvar, respectively. Thes values increased further to 2404.46 A and 2097.35 Mvar due to the 20 V/km applied geoelectric field, meaning that the effective GICs increase gradually along with the applied electric field strengths.

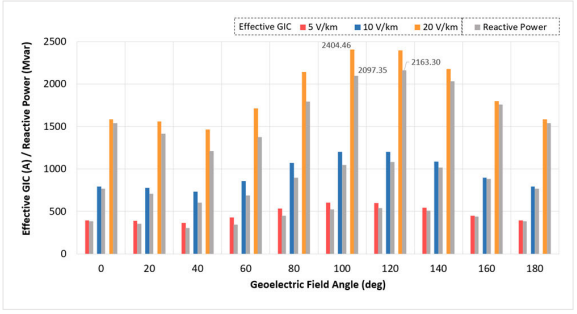

FIGURE 7. Comparison results of GIC flow and reactive power sums in all transformers available in the Malaysian power network due to the extreme electric fields directed at 0–180° angles clockwise from the North. Red, blue, and orange represent effective GIC for 5 V/km, 10 V/km, and 20 V/km geoelectric field strengths, respectively, and grey represents reactive power losses for each field.

The reactive power losses of transformers due to GICs were calculated based on Equation 6, considering different k factor values for each transformer type available in the system, as presented in Fig. 4 since it is more precise than the unity k factor for all transformers. In this case, the highest reactive power sum was obtained at a field angle of 120° with the value of 2163.30 Mvar. In Fig. 8, the results of the induced DC voltage potentials at different substations show that the induced DC voltages of substations gradually increase by increasing the magnitude of the applied geoelectric field. The polarity of induced voltages strongly depends on the locations of the substations with respect to the field direction or storm angle, as presented in Equation 1. In addition, the largest induced DC voltage will be produced if the substations or transmission lines between them are parallel to the geoelectric field with the largest GICs. In contrast, transmission lines perpendicular to the geoelectric fields result in a zero-induced voltage [20].

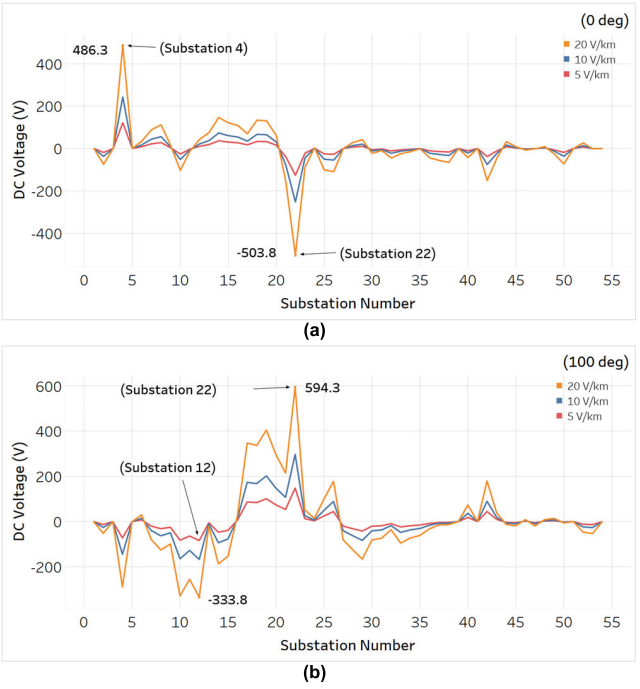

FIGURE 8. The induced DC voltage at substation ground grids in the Malaysian power network model due to the extreme electric fields at (a) 0° northward and (b) 100° eastward orientations.

In terms of calculated GICs at the substation ground grids, Figs. 9 and 10 show the performance of the Malaysian power network in the presence of extreme GMD with the value of 20 V/km at different field angles. As seen from Fig. 9, the obtained GICs range of substations at different angles were between +896 A (flowing into the system) at substation 22 and −660 A (flowing into the ground) at substation 4. Also, Figs. 9 and 10 show that substations 4, 19 and 22 experienced the peak GICs during the GIC analysis for different field angles which indicates that they may collapse due to such GMD event, the highest GICs obtained at 22 with the value of 896 A at 140°. The peak GICs were obtained at these substations because of their critical location with respect to the applied storm.

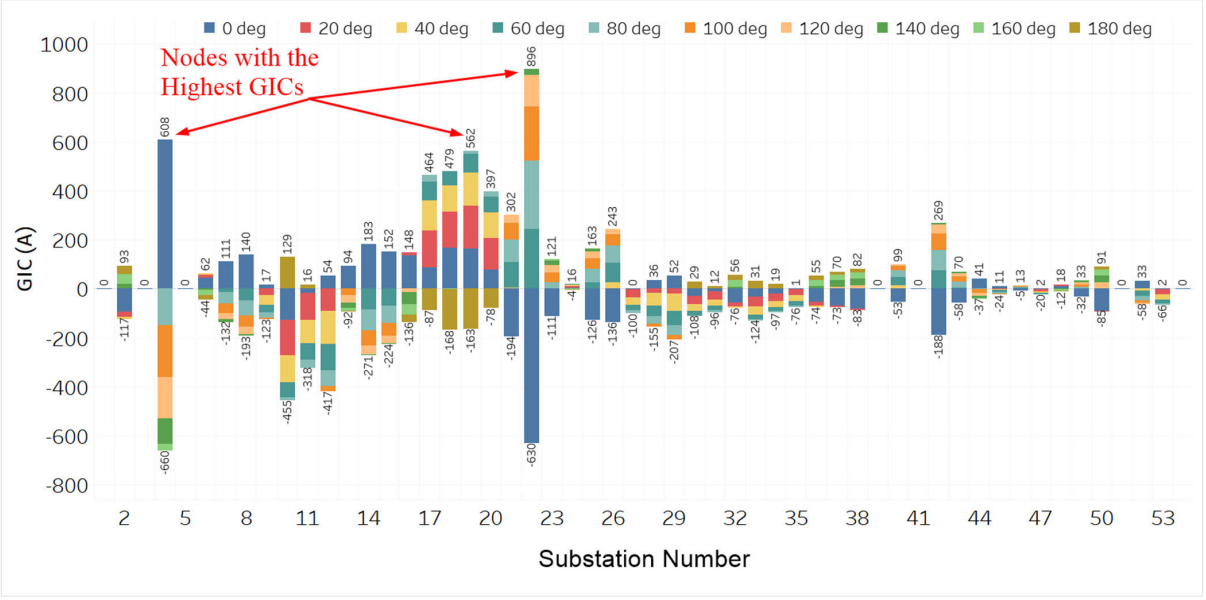

FIGURE 9. The presentation of computed GICs at the substation ground grids. The different colours indicate different orientations of the 20 V/km geoelectric field. A positive value indicates GIC (flowing from the ground into the grid) and a negative (flowing from the grid into the ground).

The results show that the GICs at a particular site remain positive or negative throughout the modelled storms for a certain angle. The GIC behaviour in the power grid depends on the different system components' resistance and the lines' induced DC voltage. The substation level GIC is the total GIC observed at the common neutral ground path of the transformers and divided based on the number of neutral grounded transformers available in the station.

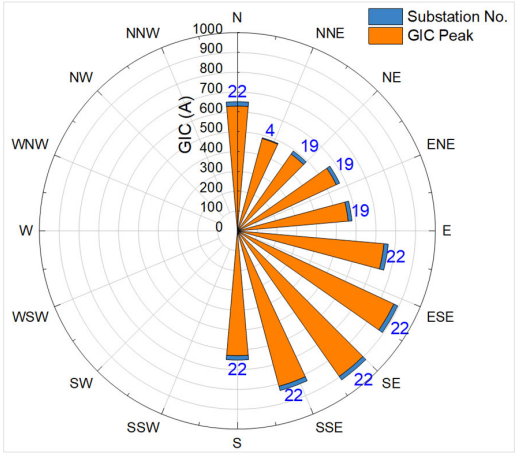

FIGURE 10. The absolute GIC peak at substation ground grids at different field orientations due to 20 V/km.

In addition, Fig. 11 shows the observed effective GIC in windings of the transformers available in the system due to 20 V/km. As can be seen from the figure, the highest per phase GIC obtained at transformer located at substation 4 with the value of 101.3 A at 0° field angle. While at 100° field angle, the highest per phase GIC obtained at transformers located at substation 19 with the value of 84.3 A. Note that this field angle also experienced the highest GIC sum with respect to all transformers in the system, as we discussed in Fig. 7.

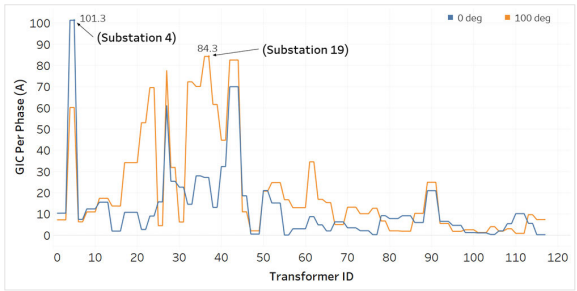

FIGURE 11. The comparison of effective GICs flow in the transformers available in the system due to 20 V/km northward (blue) and east-southward (orange) geoelectric fields. The colours indicate a different orientation angle of the 20 V/km geoelectric field.

Furthermore, to analyse the effects of substation isolation during the GMD events on the calculated GICs in the system, we gradually isolated the substation number from the system and repeated the simulations each time for 20 V/km geoelectric field at 0–180° directions, as illustrated in Fig. 12. In this work, substation isolation was selected randomly, however, in the real scenario only the most significant substations with respect to GIC response will be selected for isolation. As it is clear from the figure, increasing the number of isolated substations gradually decreases the sum of effective GIC from the system as the number of GIC flow paths is reduced. The decreasing rate varies from one field angle to another due to

GIC distribution in the system with respect to a particular field angle. Substation isolation is another technique that can be used to avoid GIC flow into the system during GMD events. However, great care must be considered as other power quality issues may arise.

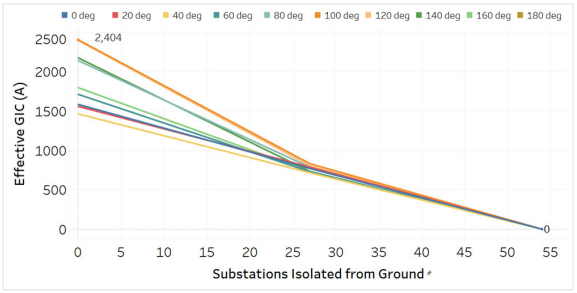

FIGURE 12. The maximum sum of effective GICs for the Malaysian power grid model as substations have their transformers isolated from the ground. The different colours indicate different orientation angles of 20 V/km geoelectric field.

B. SECOND SIMULATION CASE

The GR of the substations is one of the power network characteristics that influence the magnitude of GICs. The transformer's neutrals are connected to a mesh of conductors buried in the sediment at the substation location. If it is conductive, the substation will exhibit a low GR and higher GICs will flow into the system from the ground. Likewise, the resistive sediment will lead to a high GR, thus limiting the GICs. As a safety precaution, substations are built with the lowest possible GR values [20]. Furthermore, the IEEE standard recommends a GR value within the limit of 1 Ω in the case of transmission substation, whereas the distribution substation is recommended for a value within the limit of 5 Ω [21]. Therefore, this simulation case investigated the effect of different GRs on induced currents. Firstly, the whole system was evaluated by uniformly altering the GR of all substations with values of 0.1, 0.3, 0.6, 0.8, 1, 3, and 5 Ω.

Then, the system was evaluated with non-uniform GRs of the substations with the same range (0.1-5 Ω), as presented in Fig. 13 as it could lead to relatively different GICs in the system. The selected GR values are within the recommended GR ranges based on the IEEE standard. These values are the most actual representation of the substations' GRs in Malaysia since the Malaysian power utility follows the IEEE standard [22]. The GICs were computed individually across the system for each GR value due to 20 V/km at different directions of 0–180°. It was expected that all currents would be decreased when the GRs increased, correspondingly reducing the reactive losses as well. Note that the GR values in the first simulation case were set to 0.8 Ω. The significance of this simulation case was that it would assist utility operators in predicting the produced GICs concerning different GR resistances during space weather [23], [24], [25]. The simulation results in Figs. 14 and 15 for 0.1, 0.3, 0.6, 0.8, 1, 3, 5 Ω, and non-uniform GR values are represented in the graphs as blue, orange, grey, black, green, yellow, purple, and red, respectively. As expected, the simulation results showed that varying the GR from 0.1 up to 5 Ω recorded a significant difference in the estimated GICs and reactive power losses at most substations for 20 V/km applied geoelectric field.

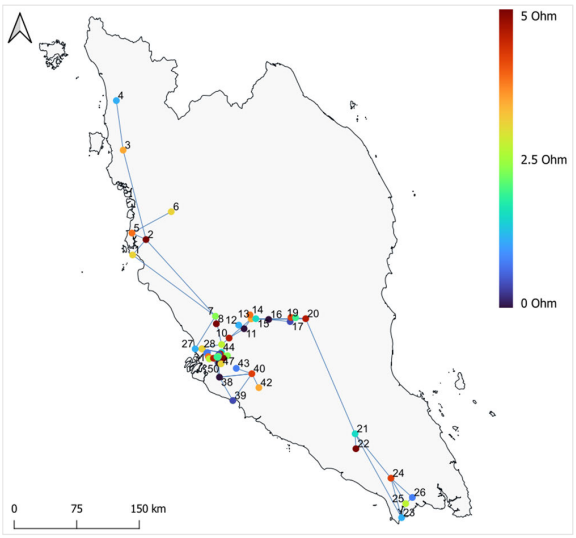

FIGURE 13. Locations of substations for non-uniform GRs with the range of 0.1–5 Ω.

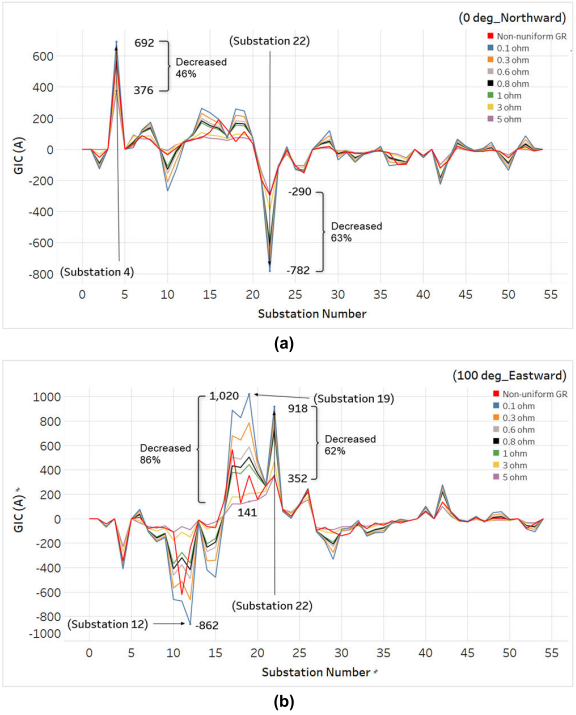

FIGURE 14. Variation of total GIC flows into the substation ground grids due to 20 V/km geoelectric fields at (a) 0° and (b) 100° field orientations under different GRs when uniformly and non-uniformly applied.

In terms of the variation of GIC flow into the substation under different GR values, Fig. 14a shows that at 0° angle, the maximum GIC produced at substation 22 with value of −782 A when the GRs of substations equal to 0.1 Ω and the 20 V/km geoelectric field. Increasing the value of GRs

decreased the produced GICs at most substations gradually and the lowest GIC values were obtained when the GR was 5 Ω. At substation 22, the GIC results decreased by 63% to −290 A due to the 20 V/km geoelectric field when the GRs were increased to 5 Ω. At 100° oriented electric field, the maximum GIC observed at substation 19 was 1020 A due to the same geoelectric field magnitude when the GRs were 0.1 Ω, as illustrated in Fig. 14b. When the GRs were increased, the GICs of most substations in the network model decreased. The GIC value at substation 19 was recorded at 141 A (decreased 86%) for the above extreme applied field when the GRs were set to 5 Ω. The results showed that the GICs at some substations varied considerably with the altering GR values, while others were only slightly varied. On the contrary, the flow of GICs was limited if the value of GRs was increased. In terms of results for non-uniform GR of the substations, Fig. 14 shows that the GIC almost have the same pattern for most of the substations, except substations 11, 18, and 19 in Fig. 14b the variation rate of GIC values is high compared to GIC results for uniformly applied GRs. Note that only the graphs for these two angles were presented to highlight the results' significance and avoid confusing readers.

Similar to the previous case, Fig. 15 shows that the highest sum of reactive power losses in all transformers in the network model due to the 20 V/km applied electric fields was obtained at 120° field direction for different GRs. Given that the maximum sum of reactive power losses obtained at 0.1 Ω was 2945.67 Mvar. The increase in GRs of the substations caused a decrease in the sum of effective GICs and reactive power losses in all transformers in the network with respect to different geoelectric field angles. The lowest sum of reactive power losses across the system at the same field angle was 1205.61 Mvar (decreased 59%) when the GRs of substations were 5 Ω at the same field angle, as illustrated in the figure.

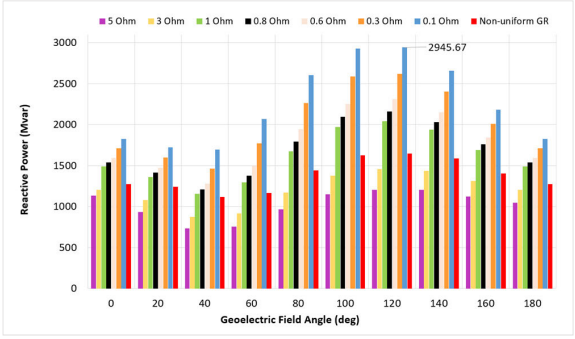

FIGURE 15. Sum of reactive power losses in all transformers available in the network model due to the 20 V/km applied geoelectric field at 0–180° field orientations under different GRs when uniformly and non-uniformly applied.

From this simulation case, we notice that the power transformers connected to the lower GR in the network system were more vulnerable to GMD events and stressed the entire system's voltage stability since they consume more reactive power losses, as presented in Fig. 15. Furthermore, the variation rates of GICs and reactive power losses depend on the value and directions of the applied geoelectric fields. For example, in Fig. 14b, the variation rate at substation 19 was 86%, which was the highest variation in this simulation case, while the variation rate at substation 22 was 62% when the GR varied from 0.1 Ω to 5 Ω. This simulation case would significantly assist the utility operators in predicting the produced GICs with respect to the different GR resistances in future GMD occurrences.

V. CONCLUSION

This work investigated the effects of extreme geoelectric fields on the Malaysian power network using the NAM method. The GICs calculated in the network model are based on various factors such as geoelectric field values, orientations, and different GRs of substations. The results showed that the sum of GIC and reactive power losses at fixed 0.8 Ω substation GRs were highest when 100° and 120° electric field angles were applied with values of 2404.46 A and 2163.30 Mvar, respectively due to the 20 V/km electric field. In terms of GICs at the substation level, the results showed that substations located in the middle of the network and connected to longer transmission lines were the most vulnerable to GMD events and experienced the most severe GIC. The maximum GIC was obtained at substation 22 with the value of 836 A at a 140° field angle with 20 V/km.

When the geoelectric field magnitudes or the number of connected substations to the system are decreased, induced voltage and GICs also decrease. Consequently, decrease the reactive power consumption of transformers. In addition, the analysis showed that an increment of GRs substations led to a limited flow of GICs, consequently minimizing the reactive power consumption. On the contrary, both the flow of GICs and reactive power losses were increased if the value of GRs were decreased. Overall, the simulation results provided new insights into the GIC effects analysis on the Malaysian power network model and HV power transformers. This could help researchers and power utilities in Southeast Asia and other low-latitude countries to predict and estimate the induced GIC during future space weather events.

ACKNOWLEDGMENT

The authors would like to acknowledge Universiti Putra Malaysia (UPM) for the technical support for this project.

REFERENCES

[1] M. Švanda, A. Smičková, and T. Výbošt'oková, "Modelling of geomagnetically induced currents in the Czech transmission grid," *Earth, Planets Space*, vol. 73, no. 1, pp. 1–11, Dec. 2021.
[2] C. T. Russell, "The solar wind interaction with the Earth's magnetosphere: A tutorial," *IEEE Trans. Plasma Sci.*, vol. 28, no. 6, pp. 1818–1830, Dec. 2000.
[3] D. M. Oliveira, D. Arel, J. Raeder, E. Zesta, C. M. Ngwira, B. A. Carter, E. Yizengaw, A. J. Halford, B. T. Tsurutani, and J. W. Gjerloev, "Geomagnetically induced currents caused by interplanetary shocks with different impact angles and speeds," *Space Weather*, vol. 16, no. 6, pp. 636–647, Jun. 2018.

[4] P. Riley, J. A. Linker, J. A. G. Esparza, L. K. Jian, C. T. Russell, and J. G. Luhmann, "Interpreting some properties of CIRs and their associated shocks during the last two solar minima using global MHD simulations," *J. Atmos. Solar-Terr. Phys.*, vol. 83, pp. 11–21, Jul. 2012.

[5] E. Matandirotya, P. J. Cilliers, R. R. Van Zyl, D. T. Oyedokun, and J. Villiers, "Differential magnetometer method applied to measurement of geomagnetically induced currents in Southern African power networks," *Space Weather*, vol. 14, no. 3, pp. 221–232, Mar. 2016.

[6] K. Burhanudin, M. H. Jusoh, Z. I. A. Latiff, M. H. Hashim, and N. D. K. Ashar, "The estimation of the geomagnetically induced current based on simulation and measurement at the power network: A bibliometric analysis of 42 years (1979–2021)," *IEEE Access*, vol. 10, pp. 56525–56549, 2022.

[7] Z. M. K. Abda, N. F. A. Aziz, M. Z. A. A. Kadir, and Z. A. Rhazali, "A review of geomagnetically induced current effects on electrical power system: Principles and theory," *IEEE Access*, vol. 8, pp. 200237–200258, 2020.

[8] P. R. Price, "Geomagnetically induced current effects on transformers," *IEEE Trans. Power Del.*, vol. 17, no. 4, pp. 1002–1008, Oct. 2002.

[9] L. Khosravi and E. Johansson, "Evaluation of the GIC module in PSS/E," M.S. thesis, Dept. Energy Environ., Chalmers Univ. Technol., Gothenburg, Sweden 2015.

[10] Z. M. Khurshid, N. F. A. Aziz, Z. A. Rhazali, and M. Z. A. A. Kadir, "Impact of geomagnetically induced currents on high voltage transformers in Malaysian power network and its mitigation," *IEEE Access*, vol. 9, pp. 167204–167217, 2021.

[11] Z. M. Khurshid, N. F. A. Aziz, Z. A. Rhazali, and M. Z. A. A. Kadir, "Effect of GIC neutral blocking devices (NBDs) on power network ferroresonance in Malaysia," *IEEE Access*, vol. 10, pp. 77225–77238, 2022.

[12] Z. M. Khurshid, N. F. A. Aziz, Z. A. Rhazali, and M. Z. A. Ab Kadir, "Geomagnetically induced current analysis in Malaysian power transmission system," *IEEE Access*, vol. 10, pp. 110205–110216, 2022.

[13] NERC. (2023). *Geomagnetic Disturbance Data*. NERC. Accessed: May 16, 2023. [Online]. Available: https://www.nerc.com/pa/RAPA/GMD/Pages/GMDHome.aspx

[14] NERC. (2017). *Reliability Standard for Transmission System Planned Performance for Geomagnetic Disturbance Events*. New Reliability Standard NERC TPL-007-1. U.S. [Online]. Available: https://assets.ccaps.umn.edu/documents/CPE-Conferences/MIPSYCON-PowerPoints/2017/TutITransmissionSystemPerformanceforGeomagneticDisturbanceEvents.pdf

[15] D. H. Boteler and R. J. Pirjola, "Modeling geomagnetically induced currents," *Space Weather*, vol. 15, no. 1, pp. 258–276, Jan. 2017.

[16] X. Dong, Y. Liu, and J. G. Kappenman, "Comparative analysis of exciting current harmonics and reactive power consumption from GIC saturated transformers," in *Proc. IEEE Power Eng. Soc. Winter Meeting. Conf.*, Jan. 2001, pp. 318–322.

[17] S. Dahman. *Modeling GMD in PowerWorld Simulator*. PowerWorld Corporation. Accessed: 2019. [Online]. Available: https://www.powerworld.com/files/G02_GMD_In_Simulator.pdf

[18] A. Pulkkinen, E. Bernabeu, J. Eichner, C. Beggan, and A. W. P. Thomson, "Generation of 100-year geomagnetically induced current scenarios," *Space Weather*, vol. 10, no. 4, Apr. 2012, Art. no. S04003.

[19] K. Patil, *Modeling and Evaluation of Geomagnetic Storms in the Electric Power System*. New York, NY, USA: International Council on Large Electric Systems (CIGRE), 2014.

[20] S. Blake, "Modelling and monitoring geomagnetically induced currents in Ireland," M.S. thesis, School Phys., Trinity College Dublin, Dublin, Ireland, 2017.

[21] *IEEE Standards Interpretation for IEEE Std 80-1986 IEEE Guide for Safety in AC Substation Grounding*, IEEE Standards Association, New York, NY, USA, 1986. [Online]. Available: https://standards.ieee.org/content/dam/ieee-standards/standards/web/documents/interpretations/80-1986_interp.pdf

[22] *TNB, Substation Design Manual (Asset Management Department, TNB Distribution Division)*, Tenaga Nasional Berhad, Kuala Lumpur, Malaysia, 2012.

[23] C. D. F. Barroso, *GIC Distribution*. Lund, Sweden: Lund Univ., Sweden, 2014.

[24] J. M. Torta, S. Marsal, and M. Quintana, "Assessing the hazard from geomagnetically induced currents to the entire high-voltage power network in Spain," *Earth, Planets Space*, vol. 66, no. 1, p. 87, Dec. 2014.

[25] K. Mukhtar, M. Ingham, C. J. Rodger, D. H. Mac Manus, T. Divett, W. Heise, E. Bertrand, M. Dalzell, and T. Petersen, "Calculation of GIC in the north island of New Zealand using MT data and thin-sheet modeling," *Space Weather*, vol. 18, no. 11, Nov. 2020, Art. no. e2020SW002580.

ZMNAKO MOHAMMED KHURSHID received the Technical Diploma degree in electrical engineering from the Kalar Technical Institute, Iraq, in 2007, the B.Eng. degree in electrical and electronic engineering from the Asia Pacific University of Technology and Innovation (APU), Malaysia, in 2015, the M.Sc. degree from Universiti Putra Malaysia (UPM), Malaysia, in 2018, and the Ph.D. degree in electrical engineering from Universiti Tenaga Nasional (UNITEN), Malaysia, in 2022. His current research interests include hybrid systems, particularly those that contain renewable energy such as PV systems and wind turbines, lightning and lightning transient effects, and geomagnetically induced current (GIC) on electrical power systems.

NUR FADILAH AB AZIZ (Member, IEEE) received the Master of Engineering degree (Hons.) in electrical engineering from the University of Southampton, U.K., in 2006, and the Ph.D. degree from Universiti Teknologi Mara, Shah Alam, in 2014. She is currently a Senior Lecturer with the Department of Electrical and Electronics Engineering, Universiti Tenaga Nasional (UNITEN), Malaysia. Her research interests include power system analysis, renewable energy, fault identification and location, distribution automation, statistical pattern recognition, artificial intelligence (AI), and machine learning applications in power systems. She is also a Graduate Member of the Board of Engineers Malaysia (BEM).

ZETI AKMA RHAZALI received the Bachelor of Electrical, Electronics and System Engineering degree from Universiti Kebangsaan Malaysia, in 1996, and the Ph.D. degree in electrical engineering from Universiti Malaysia Pahang, in 2014. From 1996 to 2001, she was a Senior Engineer (Research and Development) with vast experiences in telecommunication technologies and advancements related to mobile radio, space, and satellite communications. She was the Head of the Department of Electronic and Communication Engineering, College of Engineering, Universiti Tenaga Nasional (UNITEN), from 2018 to 2019. She is currently the Head of the Department of Engineering Foundation and Diploma Studies, College of Engineering, UNITEN. Her research interests include antenna synthesis and analyses, microwave and millimeter wave engineering as well as ionospheric communication studies. She is a member of The Institution of Engineers (IEM), Malaysia. She is a Professional Engineer (P.Eng.) registered with the Board of Engineers (BEM) Malaysia.

MOHD ZAINAL ABIDIN AB KADIR (Senior Member, IEEE) received the B.Eng. degree in electrical and electronic engineering from Universiti Putra Malaysia and the Ph.D. degree in high voltage engineering from The University of Manchester, U.K. He is currently a Strategic Hire Professor with the Institute of Power Engineering (IPE), Universiti Tenaga Nasional (UNITEN), and a Professor with the Faculty of Engineering, Universiti Putra Malaysia. He is also the Founding Director of the Centre for Electromagnetic and Lightning Protection Research (CELP), Universiti Putra Malaysia. To date, he has authored or coauthored over 350 journal articles and conference papers. His research interests include high voltage engineering, lightning protection, electromagnetic compatibility, power system transients, and renewable energy. He is also an Advisory Board Member of the National Lightning Safety Institute (NLSI), USA, and a Research Advisor of the African Centre for Lightning and Electromagnetic (ACLE). He is the Chairperson of the National Mirror Committee of IEC TC 81 (Lightning Protection) and a Local Convener of MNC-CIGRE C4 on System Technical Performance. He is a Professional Engineer (P.Eng.), a Chartered Engineer (C.Eng.), and a Professional Technologist (P.Tech.). He is also an IEEE Power & Energy Society (PES) Distinguished Lecturer in the field of lightning and high voltage engineering.